

Nano SIMS characterization of boron- and aluminum-coated $\text{LiNi}_{1/3}\text{Co}_{1/3}\text{Mn}_{1/3}\text{O}_2$ cathode materials for lithium secondary ion batteries

Tae Eun Hong · E. D. Jeong · S. R. Baek ·
M. R. Byeon · Young-Suck Lee · F. Nawaz Khan ·
Ho-Soon Yang

Received: 2 September 2011 / Accepted: 4 November 2011 / Published online: 7 December 2011
© Springer Science+Business Media B.V. 2011

Abstract The $\text{LiNi}_{1/3}\text{Co}_{1/3}\text{Mn}_{1/3}\text{O}_2$ powders required for the present study, obtained by coprecipitation method has been surface coated with boron and aluminum. The morphology and crystal structure of powders have been characterized using scanning electron microscopy, X-ray diffraction and X-ray photoelectron spectroscopy techniques. The elemental distribution of the coated samples analyzed by transmission electron microscopy images and nano secondary ion mass spectrometry indicates a thin uniform layer of $[\text{B}, \text{Al}]_2\text{O}_3$ on the surface of spherical $\text{LiNi}_{1/3}\text{Co}_{1/3}\text{Mn}_{1/3}\text{O}_2$. The surface-modified $\text{LiNi}_{1/3}\text{Co}_{1/3}\text{Mn}_{1/3}\text{O}_2$ has been explored as a cathode material for lithium secondary ion battery applications. The electrochemical charge–discharge results reveal that the capacity retention rate of coated $\text{LiNi}_{1/3}\text{Co}_{1/3}\text{Mn}_{1/3}\text{O}_2$ after 40 cycles at 1 C rate maintains 93% of the initial discharge capacity while the rate of bare $\text{LiNi}_{1/3}\text{Co}_{1/3}\text{Mn}_{1/3}\text{O}_2$

maintains only 88%. It is noticed that the small amounts of boron and aluminum coatings on the surface of $\text{LiNi}_{1/3}\text{Co}_{1/3}\text{Mn}_{1/3}\text{O}_2$ can significantly improve the electrochemical properties of electrode materials because of the suppression of reaction between the cathode and the electrolytes.

Keywords Lithium secondary ion battery · Cathode material · Lithium-nickel-cobalt-manganese oxide · Electrochemical properties · Nano secondary ion mass spectrometry

1 Introduction

Recently, rechargeable lithium-ion batteries have found their way into portable electronic devices and in other fields including automotive applications [1–5]. Rechargeable lithium-ion batteries have mainly utilized the LiCoO_2 as the cathode material because of the simplicity of production and stable cycling performance [6]. However, LiCoO_2 has its own limitation due to the toxicity and the high cost of cobalt, and the poor thermal stability when it is fully charged. In search of highly improved cathode materials for the lithium-ion battery applications, various systems, such as carbon-coated LiFePO_4 cathode [7], Al_2O_3 - and AlF_3 -coated LiFePO_4 cathode [8], chitosan-added LiFePO_4 cathode [9], and LiCoO_2 cathodes [10, 11], are reported.

The $\text{LiNi}_{1/3}\text{Co}_{1/3}\text{Mn}_{1/3}\text{O}_2$ materials have been recently utilized as an alternative substitute to conventional LiCoO_2 cathodes in lithium battery applications because of their advantages, such as high capacity [6, 12], relatively good rate capability [13, 14], and enhanced safety [15–18]. However, the insufficient rate capability still limits their further applications. The studies of these mixed transition

T. E. Hong · E. D. Jeong · S. R. Baek · M. R. Byeon
Busan Center, Korea Basic Science Institute,
Busan 618-230, Korea

T. E. Hong (✉) · H.-S. Yang
Department of Physics, Pusan National University,
Busan 609-735, Korea
e-mail: tehong@kbsi.re.kr

H.-S. Yang
e-mail: hsyang@pusan.ac.kr

Y.-S. Lee
Interdisciplinary School of Green Energy, Ulsan National
Institute of Science and Technology, Ulsan 689-798, Korea

F. N. Khan
School of Advanced Sciences, VIT University,
Tamil Nadu 632-014, India

metal oxides reveal that only the trivalent cobalt plays a more active redox role in the later stages of lithium removal than the divalent nickel and the tetravalent manganese, by virtue of its being predominantly electrochemically active. However, all these layered oxides have their inherent thermodynamic instabilities upon lithium removal; hence, their kinetic instabilities can create problems if there is any thermal excursion in the electrochemical cell. The stability can, however, be improved with aluminum substitution.

There are several methods of improving the electrochemical properties of electroactive materials, such as covering electrode material surfaces with conductive surface coating [19–24], and doping with metals which improves the stability of electrode by rising electronic conductivity, and deflating polarization [25–32]. Since the energy density of batteries is very sensitive to the particle shape and size of cathode materials, it is believed that the surface coating is a useful and easy way to improve the electrochemical properties of cathode materials [19–24]. Many investigations have reported that surface-coating approach is an effective way to improve the electrochemical properties of cathode materials [16, 17]. Based on the facts mentioned above, the present study envisions the coating electroactive materials, $\text{LiNi}_{1/3}\text{Co}_{1/3}\text{Mn}_{1/3}\text{O}_2$, with a trivalent oxide of $[\text{B}, \text{Al}]_2\text{O}_3$ for the enhancement of electrochemical properties. In this study, the surface modification using boron and aluminum elements to stabilize the surface of $\text{LiNi}_{1/3}\text{Co}_{1/3}\text{Mn}_{1/3}\text{O}_2$ has been explored. $\text{LiNi}_{1/3}\text{Co}_{1/3}\text{Mn}_{1/3}\text{O}_2$ powder has been obtained by coprecipitation method, and the effect of the surface modification of $\text{LiNi}_{1/3}\text{Co}_{1/3}\text{Mn}_{1/3}\text{O}_2$ powders is discussed.

2 Experimental

The $(\text{Ni}_{1/3}\text{Co}_{1/3}\text{Mn}_{1/3})(\text{OH})_2$ has been prepared from NiSO_4 , CoSO_4 , and CoSO_4 by coprecipitation [18, 33–36]. The obtained $(\text{Ni}_{1/3}\text{Co}_{1/3}\text{Mn}_{1/3})(\text{OH})_2$ powders were then dried at 120 °C for 12 h. In order to prepare the $\text{LiNi}_{1/3}\text{Co}_{1/3}\text{Mn}_{1/3}\text{O}_2$ powder, the $(\text{Ni}_{1/3}\text{Co}_{1/3}\text{Mn}_{1/3})(\text{OH})_2$ and Li_2CO_3 at a molar ratio of 1:1.03 were mixed thoroughly and heated to 900 °C for 10 h in air. The surface of $\text{LiNi}_{1/3}\text{Co}_{1/3}\text{Mn}_{1/3}\text{O}_2$ corresponding to 0.2 mol was coated with boron (B) and aluminum (Al) by mixing 0.1 mol of the aluminum isopropoxide and 0.03 mol of boron trifluoride diethyl etherate dissolved in 100 ml of ethanol at ambient condition. It was then dried at 100 °C for 6 h and heated up to 700 °C for 10 h. The morphology and crystal structure of the coated $\text{LiNi}_{1/3}\text{Co}_{1/3}\text{Mn}_{1/3}\text{O}_2$ powders were characterized using a scanning electron microscope (SEM; Nano-Sem 230, USA), X-ray diffractometry (XRD; Rigaku D/Max-2200V, Japan) X-ray photoelectron spectrometer

(XPS; Escalab 250, UK) and transmission electron microscopy (TEM; JEM2011, Japan).

Nano secondary ion mass spectrometry equipped with a cesium gun (Nano SIMS; Cameca Nano-SIMS 50, France) having spatial resolution of 50 nm which is superior to other dynamic SIMS is employed to analyze the composition and spatial distribution of elements on the surface and the cross section of materials. The experimental data were obtained in multi collection detector mode by sputtering the sample with a ~ 1 pA Cs^+ primary ion beam focused into a spot of ~ 100 nm diameter. The primary ion beam was rastered over $20 \times 20 \mu\text{m}^2$. Samples were coated with gold for charge compensation, and a pre-sputtering of the surface was performed before any measurements to remove the surface contamination of gold-coated layer. The powders were also mounted using epoxy resin and then polished with SiC paper to measure the element distribution on the cross section of the coated $\text{LiNi}_{1/3}\text{Co}_{1/3}\text{Mn}_{1/3}\text{O}_2$ powders.

The charge–discharge characteristics of $\text{LiNi}_{1/3}\text{Co}_{1/3}\text{Mn}_{1/3}\text{O}_2$ cathodes have been investigated in CR2016 coin-type half cells. The coin-type half cell 2016-size contained a test electrode, a lithium-metal counter-and-reference electrode, a 15- μm -thick microporous polyethylene separator, and an electrolyte solution of 1.15 M LiPF_6 in ethylene carbonate (EC)/dimethyl carbonate (DMC)/diethyl carbonate (DEC) (3:4:3 vol.%) (LG Chem., Korea). The amount of active materials in the cathode composite was 20 mg. The cathodes for the battery test cell were made from the cathode materials, super P carbon black, and polyvinylidene fluoride (PVdF) binder (Solef) in a weight ratio of 94:3:3. The electrodes were prepared by coating a cathode-slurry onto an Al foil followed by drying at 130 °C for 20 min, and finally subjected to a roll-pressing.

3 Results and discussion

Figure 1a, b represent the SEM images of the bare and the surface-coated $\text{LiNi}_{1/3}\text{Co}_{1/3}\text{Mn}_{1/3}\text{O}_2$, respectively. The bare $\text{LiNi}_{1/3}\text{Co}_{1/3}\text{Mn}_{1/3}\text{O}_2$ powders show round shapes with the 10–15 μm size. The SEM images reveal the surface-coated $\text{LiNi}_{1/3}\text{Co}_{1/3}\text{Mn}_{1/3}\text{O}_2$ remains unaltered even after the surface-coating process, but the particle size is increased by about 1 μm .

The XRD patterns of the bare and the surface-coated $\text{LiNi}_{1/3}\text{Co}_{1/3}\text{Mn}_{1/3}\text{O}_2$ powders are presented in Fig. 2a, b, respectively. All the observed diffraction lines correspond to those of a $\alpha\text{-NaFeO}_2$ layered structure with a space group of $R\bar{3}m$ [37–40]. The lattice parameter a obtained from Fig. 2 is 2.863 Å for the both samples, and the calculated lattice parameter c is 14.242 and 14.260 Å for the bare and the coated $\text{LiNi}_{1/3}\text{Co}_{1/3}\text{Mn}_{1/3}\text{O}_2$, respectively. These results suggest that the crystal structure of $\text{LiNi}_{1/3}$

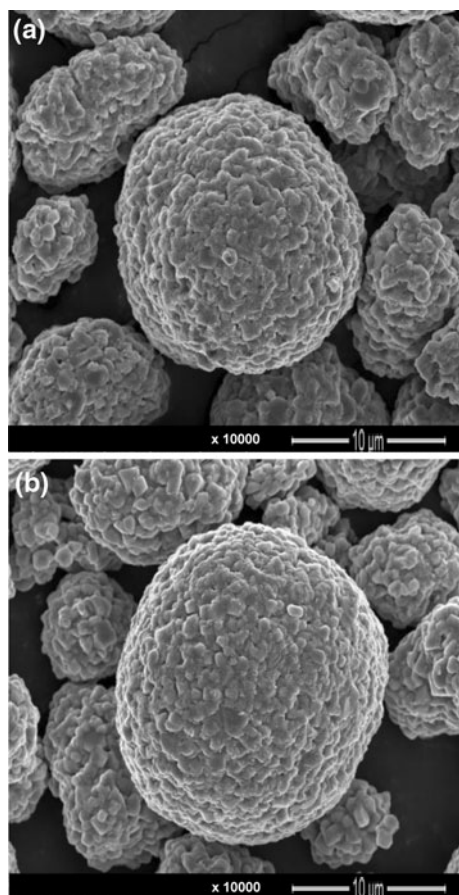


Fig. 1 SEM images of (a) bare and (b) $[B, Al]_2O_3$ -coated $LiNi_{1/3}Co_{1/3}Mn_{1/3}O_2$ powder

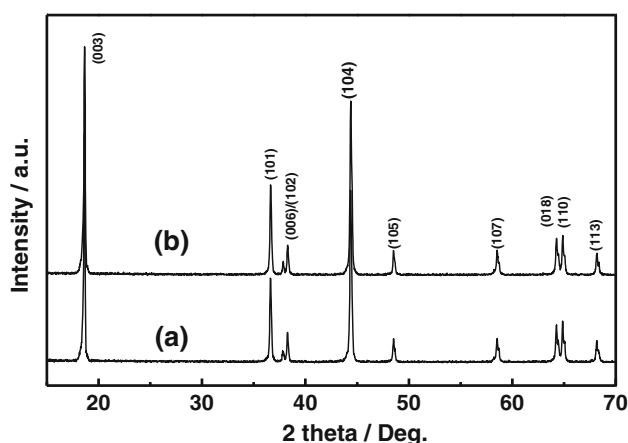


Fig. 2 X-ray diffraction patterns of (a) bare and (b) $[B, Al]_2O_3$ -coated $LiNi_{1/3}Co_{1/3}Mn_{1/3}O_2$

$Co_{1/3}Mn_{1/3}O_2$ is not affected significantly by the surface coating.

The Ni and Mn distributions as well as those of boron and aluminum were examined by means of Nano SIMS 50

having spatial resolution of 100 nm. Figure 3a, b shows the elemental distributions (B, Al, Ni, and Mn) on the surface and the cross section of the surface-coated $LiNi_{1/3}Co_{1/3}Mn_{1/3}O_2$ powders, respectively. The distributions of B and Al elements are given in the left and the right images, respectively, at the top in each of (a) and (b), and reveal that these elements are distributed only on the surface of the $LiNi_{1/3}Co_{1/3}Mn_{1/3}O_2$. The chemical composition of boron and aluminum elements on the surface was explored by X-ray photoelectron spectroscopy measurements (Fig. 4). The core-level spectra analysis reveals that the boron forms B_2O_3 and aluminum forms Al_2O_3 . Nano SIMS images on the cross section of the surface-coated $LiNi_{1/3}Co_{1/3}Mn_{1/3}O_2$ powders show that the thickness of coated layer is about 0.7 μm . The distribution of Ni and Mn elements given in the left and the right images, respectively, at the bottom in each of (a) and (b) show that Ni and Mn elements are distributed uniformly throughout the $LiNi_{1/3}Co_{1/3}Mn_{1/3}O_2$ particles as desired. It is worth to mention that in enhancing the electrochemical properties, it is important to have dense coating. In Fig. 3b, the Nano SIMS image shows that the coverage of the coating is uniformly distributed throughout the entire surface, even though there is slight variation of the intensity of the coated material. Furthermore, TEM observation (Fig. 5) also showed the existence of the the fully covered dense coating.

The capacity–voltage curves for the first cycle of the bare and surface-coated $LiNi_{1/3}Co_{1/3}Mn_{1/3}O_2$, respectively, as the cell voltages are changed from 3.0 to 4.5 V at a constant current density, are shown in Fig. 6a, b. The curves were obtained at the charge–discharge rates of 0.1, 0.2, 0.5, and 1.0 C for each sample. The discharge capacities of the bare $LiNi_{1/3}Co_{1/3}Mn_{1/3}O_2$ corresponding to 0.1, 0.2, 0.5, and 1.0 C were 181, 177, 166 and 152 $mAhg^{-1}$, respectively. Similar to the bare sample, the surface-coated $LiNi_{1/3}Co_{1/3}Mn_{1/3}O_2$ exhibits the discharge capacities of 182, 177, 163, and 149 $mAhg^{-1}$ corresponding to 0.1, 0.2, 0.5 and 1 C, respectively. Previously, Huang et al. [37] reported that the initial discharge-specific capacities in $LiNi_{1/3}Co_{1/3}Mn_{1/3}O_2$ at 0.1, 0.5, 1, and 2 C were 153, 140, 130 and 118 $mAhg^{-1}$, respectively. The discharge capacities of the both samples are significantly improved compared with the previous reported results of $LiNi_{1/3}Co_{1/3}Mn_{1/3}O_2$ materials [38–40].

Figure 7 shows the capacity as a function of cycle numbers for the bare and the surface-coated $LiNi_{1/3}Co_{1/3}Mn_{1/3}O_2$. As the cycle of charge–discharge repeats at a rate of 1.0 C, the discharge capacity decreases. However, the variation of capacity as the number of cycle increases is different between the bare and surface-coated $LiNi_{1/3}Co_{1/3}Mn_{1/3}O_2$ powders. The retention capacity of bare $LiNi_{1/3}Co_{1/3}Mn_{1/3}O_2$ after 40 cycles is 88% of initial capacity, but the retention capacity of the surface-coated $LiNi_{1/3}Co_{1/3}Mn_{1/3}O_2$ is 92% of initial capacity.

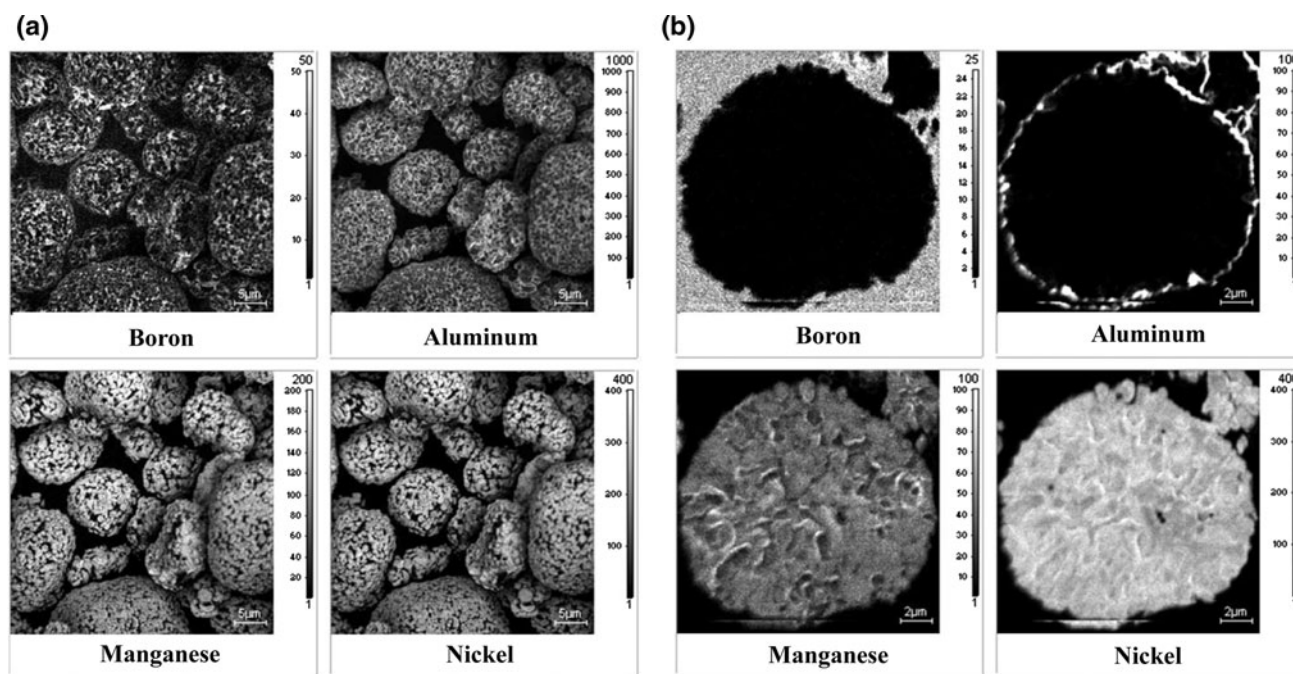


Fig. 3 Elemental distributions of B, Al, Mn, and Ni on (a) the surface and (b) the cross section of $[\text{B}, \text{Al}]_2\text{O}_3$ -coated $\text{LiNi}_{1/3}\text{Co}_{1/3}\text{Mn}_{1/3}\text{O}_2$ obtained by Nano SIMS. The *left* and the *right* images at the top in

both (a) and (b) are the distributions of B and Al, respectively, and the *left* and the *right* images at the bottom are the distributions of Mn and Ni, respectively

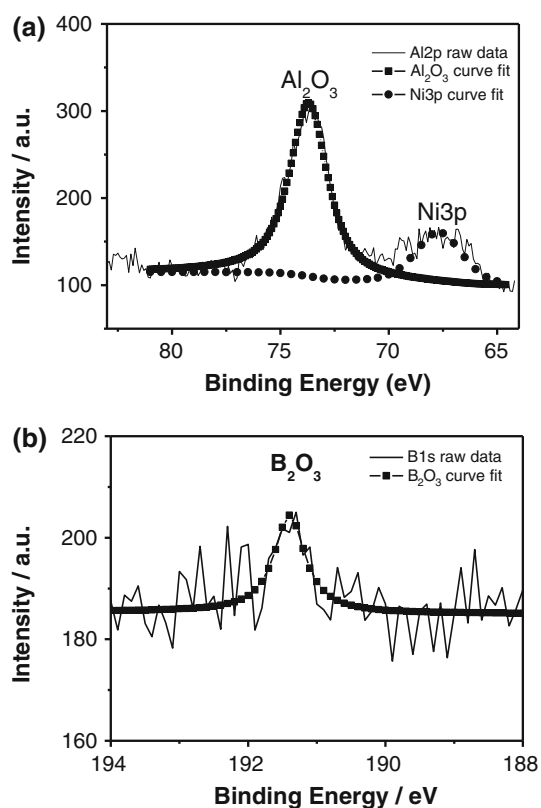


Fig. 4 X-ray photoelectron spectra of (a) B1s and (b) Al2p on the surface of $[\text{B}, \text{Al}]_2\text{O}_3$ -coated $\text{LiNi}_{1/3}\text{Co}_{1/3}\text{Mn}_{1/3}\text{O}_2$

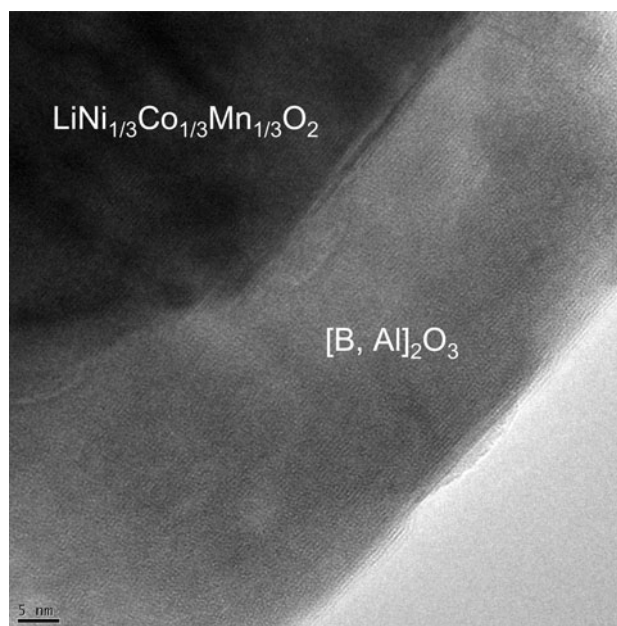


Fig. 5 Transmission electron microscopy image of $[\text{B}, \text{Al}]_2\text{O}_3$ -coated $\text{LiNi}_{1/3}\text{Co}_{1/3}\text{Mn}_{1/3}\text{O}_2$

$\text{Mn}_{1/3}\text{O}_2$ improves to 93%. Even though there is no significant difference in the irreversible capacity loss between the bare and the surface-coated $\text{LiNi}_{1/3}\text{Co}_{1/3}\text{Mn}_{1/3}\text{O}_2$.

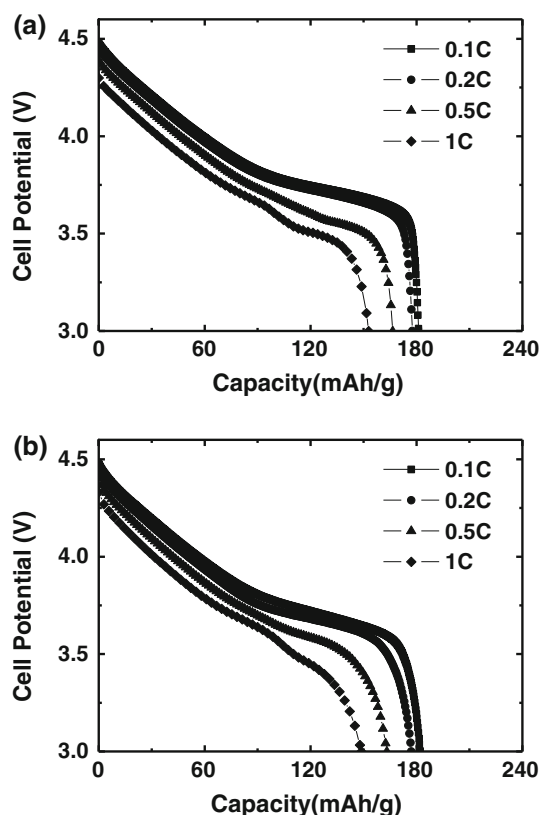


Fig. 6 Capacity–voltage curves of (a) bare $\text{LiNi}_{1/3}\text{Co}_{1/3}\text{Mn}_{1/3}\text{O}_2$ (b) $[\text{B}, \text{Al}]_2\text{O}_3$ -coated $\text{LiNi}_{1/3}\text{Co}_{1/3}\text{Mn}_{1/3}\text{O}_2$ for the initial cycle at the charge–discharge rates of 0.1, 0.2, 0.5, and 1.0 C

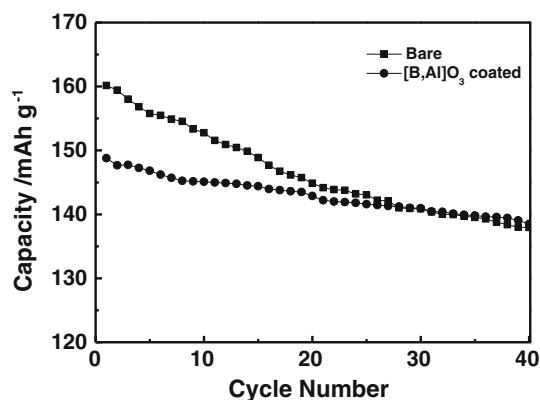


Fig. 7 Cycle performances of bare $\text{LiNi}_{1/3}\text{Co}_{1/3}\text{Mn}_{1/3}\text{O}_2$ and $[\text{B}, \text{Al}]_2\text{O}_3$ -coated $\text{LiNi}_{1/3}\text{Co}_{1/3}\text{Mn}_{1/3}\text{O}_2$ at a 1.0 C rate in lithium half cells

4 Conclusions

Spherical $\text{LiNi}_{1/3}\text{Co}_{1/3}\text{Mn}_{1/3}\text{O}_2$ powders forming in a $\alpha\text{-NaFeO}_2$ crystal structure were synthesized with coprecipitation method. The surface of $\text{LiNi}_{1/3}\text{Co}_{1/3}\text{Mn}_{1/3}\text{O}_2$ powder was coated successfully with boron and aluminum. The thin and uniform $[\text{B}, \text{Al}]_2\text{O}_3$ layer is observed on the surface of

$\text{LiNi}_{1/3}\text{Co}_{1/3}\text{Mn}_{1/3}\text{O}_2$ by Nano SIMS. There is significant improvement in the initial discharge specific capacities of both bare $\text{LiNi}_{1/3}\text{Co}_{1/3}\text{Mn}_{1/3}\text{O}_2$ and $[\text{B}, \text{Al}]_2\text{O}_3$ -coated $\text{LiNi}_{1/3}\text{Co}_{1/3}\text{Mn}_{1/3}\text{O}_2$ compared with the results of others. Although the coated $\text{LiNi}_{1/3}\text{Co}_{1/3}\text{Mn}_{1/3}\text{O}_2$ has no significant difference in initial discharge capacity, the capacity retention is improved compared with bare $\text{LiNi}_{1/3}\text{Co}_{1/3}\text{Mn}_{1/3}\text{O}_2$. The enhancement of retention capacity is attributed to the improvement in the charge transfer kinetics and the stability in electrolyte due to $[\text{B}, \text{Al}]_2\text{O}_3$ coating. We confirm that a thin coating of boron and aluminum on surface of $\text{LiNi}_{1/3}\text{Co}_{1/3}\text{Mn}_{1/3}\text{O}_2$ can significantly improve the electrochemical properties as an electrode material.

Acknowledgment This study was supported by KBSI Grant (T31601) to T. E. Hong.

References

- Scrosati B (1995) *Nature* 373:557
- Tarascon JM, Armand M (2001) *Nature* 414:359
- Guyomard D (2000) New trends in electrochemical technology: energy storage systems for electronics. Gordon & Breach Science Publishers, New York
- Wakihara W, Yamamoto O (1998) Lithium ion batteries—fundamentals and performance. Kodansha-Wiley-VCH, Weinheim
- Bruce PG, Scrosti B, Tarascon JM (2008) *Angew Chem Int Ed* 47:2930
- Antolini E (2004) *Solid State Ionics* 170:159
- Jeong ED, Kim HJ, Ahn CW, Ha MG, Hong TE, Kim HG, Jin JS, Bae JS, Hong KS, Kim YS, Kim HJ, Doh CH, Yang HS (2009) *J Nanosci Nanotechnol* 9:4467
- Ahn CW, Ha MG, Hong KS, Lee DJ, Doh CH, Doh KY, Na JM, Song BH, Jeon HM, Cho YG, Yang HS, Jeong ED (2010) *Defect Diffus Forum* 297:906
- Hong KS, Yu SM, Ha MG, Ahn CW, Hong TE, Jin JS, Kim HG, Jeong ED, Kim YS, Kim HJ, Doh CH, Yang HS, Jung H (2009) *Bull Korean Chem Soc* 30:1719
- Cho PJ, Jeong ED, Shim YB (1998) *Bull Korean Chem Soc* 19:39
- Jeong ED, Won MS, Shim YB (1998) *J Power Sources* 70:70
- Stewart SG, Srinivasan V, Newman J (2008) *J Electrochem Soc* 155:A664
- He SS, Ma ZF, Liao XZ, Jiang Y (2007) *J Power Sources* 163:1053
- Martha SK, Markevich E, Burgel V, Salitra G, Zingirad E, Markovsky B, Sclar H, Pramovich Z, Heik O, Aurbach D, Exnar I, Buqa H, Drezen T, Semrau G, Schmidt M, Kovacheva D, Saliyski N (2009) *J Power Sources* 189:288
- Martha SK, Sclar H, Framowitz ZS, Kovacheva D, Saliyski N, Gofer Y, Sharon P, Golik E, Markovsky B, Aurbach D (2009) *J Power Sources* 189:248
- Ohzuku T, Makimura Y (2001) *Chem Lett* 7:642
- Yabuuchi N, Ohzuku T (2003) *J Power Sources* 119:171
- Kim J, Park C, Sun Y (2003) *Solid State Ionics* 164:43
- Huang SH, Wen ZY, Zhang JC, Gu ZH, Xu XH (2006) *Solid State Ionics* 177:851
- Dominko R, Gaberscek M, Bele U, Mihailovic D, Jamnik J (2007) *J Eur Ceram Soc* 27:909
- Liu H, Feng Y, Wang K, Xie JY (2008) *J Phys Chem Solids* 69:2037
- Huang JJ, Jiang ZY (2008) *Electrochim Acta* 53:7756

23. Yang LZ, Gao LJ (2009) *J Alloys Comp* 485:93
24. Wolfenstine J, Lee U, Allen JL (2006) *J. Power Sources* 154:287
25. Liu DT, Quyang CY, Shu J, Jiang J, Wang ZX, Chen LQ (2006) *Phys Stat Sol (b)* 243:1935
26. Hao YJ, Lai QY, Lu JZ, Ji XY (2007) *Ionics* 13:369
27. Kubiak P, Garcia A, Womes M, Aldon L, Olivier-Fourcade J, Lippens PE, Jumas JC (2003) *J Power Sources* 119:626
28. Huang SH, Wen ZY, Gu ZH, Zhu XJ (2005) *Electrochim Acta* 50:4057
29. Huang SH, Wen ZY, Zhu XJ, Lin ZX (2007) *J Power Sources* 165:408
30. Yu HY, Zhang XF, Jalbout AF, Yan XD, Pan XM, Xie HM, Wang RS (2008) *Electrochim Acta* 53:4200
31. Tabuchi T, Yasuda H, Yamachi M (2006) *J Power Sources* 162:813
32. Wolfenstine J, Allen JL (2008) *J Power Sources* 180:582
33. Wu Y, Manthiram A (2009) *Solid State Ionics* 180:50
34. Liu J, Manthiram A (2009) *Chem Mater* 21:1695
35. Lee MH, Kang YJ, Myung ST, Sun YK (2004) *Electrochim Acta* 50:939
36. Cho TH, Park SM, Yoshio M (2004) *Chem Lett* 700
37. Huang ZD, Liu XM, Zhang B, Oh S, Ma PC, Kim JK (2011) *Scripta Mater* 64:122
38. Kim GH, Myung ST, Kim HS, Sun YK (2006) *Electrochim Acta* 51:2447
39. Chang Z, Chen Z, Wu F, Tang H, Zhu Z, Yuan ZZ, Wang H (2008) *Electrochim Acta* 53:5927
40. Zhang S, Deng C, Fu BL, Yang SY, Ma L (2010) *Powder Technol* 198:373